TS-fuzzy controller for UPFC in a multimachine power system

S.Mishra, P.K.Dash and G.Panda

Abstract: The unified power flow controller is one of the most versatile flexible AC transmission system devices, which can be used to control the active and reactive power flows in a transmission line by injecting a variable voltage in series and reactive current in shunt. The application of Takagi-Sugeno type fuzzy logic controllers for UPFC voltage source inverter control in a multi-machine power system environment is proposed. This type of fuzzy controller provides a wide range of control gain variation by including both linear and non-linear terms in the consequent part of the fuzzy rule base. The TS fuzzy controllers are quite general in that they use arbitrary input fuzzy sets, any type of fuzzy logic, and the general defuzzifier. Several computer simulation tests on a multi-machine power system indicate the significant damping performance of this new TS fuzzy controller for the UPFC.

1 Introduction

The concept of the flexible AC transmission system (FACTS) envisages the use of solid state controllers to achieve flexibility of power system operation by fast and reliable control. One of the greatest advantages of using a FACTS device in a power transmission system is to enhance the transient stability performance of the system by controlling the real and reactive power flow of the line during fault conditions. The unified power flow controller (UPFC) is one of the most versatile of the FACTs controllers [1] and its main function is to inject a controllable series voltage (both in magnitude and phase angle with respect to the bus where it is located) thereby modulating the line reactance and controlling the power flow in the transmission line. Two voltage source inverters connected by a capacitor charged to a DC voltage realise the UPFC. The converter number one, which is a shunt converter, draws real power from the source and exchanges it (minus the losses) to the series converter. The power balance between the shunt and series converters is maintained, to keep the voltage across the DC link capacitor constant.

As the UPFC can provide a smooth control response, an analytical model that neglects the switching details is adequate to study low frequency electromechanical oscillations. To control the magnitude and phase angle of the injected voltage source, the in-phase and quadrature component of the voltage (with reference to the line current) are controlled using the PI regulator (conventional control) [2]. The real and reactive power references are used for this control and are derived from steady state power flow requirements. The shunt converter of the UPFC may be controlled to provide the DC capacitor voltage constant along with the bus voltage regulation. This is achieved by controlling the in-phase and quadrature components of the shunt current (with respect to the system bus voltage where the UPFC is located) using PI regulators.

It is well known that the PI regulators cannot perform satisfactorily in damping electromechanical oscillations over a wide range of power system operating conditions. The fuzzy logic control has been successfully applied for synchronous generator excitation control [3–5], control of static VAr systems [6], series reactance switching control [7] and the series and shunt voltage source converter control for the UPFC [8]. The fuzzy logic approach provides the design of a non-linear model free controller and is capable of coordinating the performance of series and shunt converter controllers. The Mamdani type [8] fuzzy logic controller presented for UPFC may not be able to provide a wide variation of control gains for the UPFC to operate either as an impedance compensator, phase-angle controller or a voltage regulator. Instead a Takagi-Sugeno type fuzzy controller [9] can provide a wide range of control gain variation and can use both linear and non-linear rules in the consequent expression of the fuzzy rule base. As new methods have been outlined for the design of TS fuzzy controllers, the purpose of this paper is to highlight the application of TS fuzzy controllers to provide regulation of the series and shunt voltage source inverter of the UPFC, in a multi-machine environment. The simulation results presented highlight the effectiveness of the TS-fuzzy controller in damping inter-area and local mode oscillations of the multi-machine power system.

2 System model

A multi-machine power system as shown in Fig. 1 is simulated representing the synchronous generator by a 3rd order model. Each generator is equipped with a simple automatic voltage regulator (AVR). The differential equations governing the dynamics of the machine are given in Appendix 1. No damper winding is modelled, as we are investigating the performance of the UPFC controller. The second machine (M-2) is equipped with a conventional power system stabiliser (PSS) to damp out the small oscillations in the local mode.

IEE Proceedings online no. 20000022

DOI: 10.1049/ip-gtd:20000022

Paper received 16th April 1999

The authors are with the Regional Engineering College, Rourkela, India

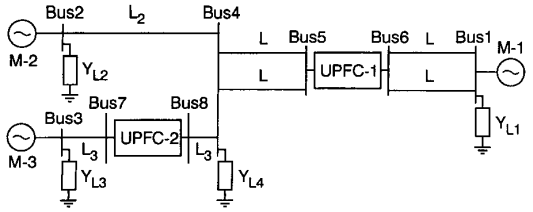

Fig. 1 *500kV multi-machine power system*

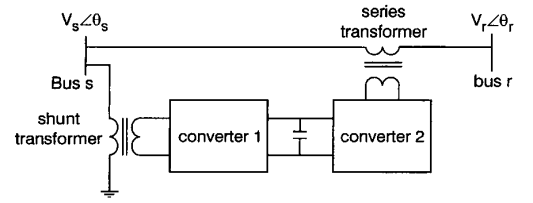

Fig. 2 *Basic arrangement for UPFC*

2.1 UPFC model

The UPFC is one of the most versatile FACTS devices, and controls the real and reactive power flow in the line independently by using the series injected voltage. It should be noted that the UPFC uses voltage source converters (VSCs) for series voltage injection as well as shunt current control. The injected series voltage can be split into two components that are in phase (real voltage) and in quadrature (reactive voltage) with the line current. Varying the series reactance of the line can effectively control the real power. The two voltage source converters (converter-1 and converter-2) are connected via a common DC link capacitor as shown in Fig. 2. The function of the shunt converter is to circulate the real power demand of the series converter through the DC link. The two converters can draw or inject reactive power to the system independently. The UPFC injection model with exact real power balance between the converters is already given in literature [10]. The detailed model is derived in Appendix 2. The assumption of exact power balance between Converter-1 and Converter-2 is never realisable in actual practice as the two converters are independently controlled. Thus the injection model is modified to take care of the mismatch in real power.

Let a current I_s in phase with the voltage V_s be drawn by the shunt converter. The real power of converter-1 is

$$P_{conv1} = |V_s|.I_s \tag{1}$$

This is added to the real power drawn, at the bus s, of the series voltage source injection model depicted in Fig. 28 in Appendix 2. Thus the new injection model is shown in Fig. 3. ρ is defined as $|V_c|/|V_s|$ and α is the phase difference between V_c and V_s.

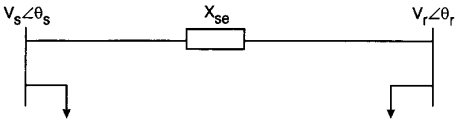

Fig. 3 *UPFC injection model*
$P_s = \rho B_{se}|V_s|^2 \sin(\alpha) + |V_s|.I_s$ $\quad P_r = -\rho B_{se}|V_s|.|V_r| \sin(\theta_{sr} + \alpha)$
$Q_s = \rho B_{se}|V_s|^2 \cos(\alpha)$ $\quad Q_r = -\rho B_{se}|V_s|.|V_r| \cos(\theta_{sr} + \alpha)$

Due to the mismatch of real power between the two converters the DC link capacitor voltage is not constant. The dynamics of the DC voltage neglecting losses can be represented by

$$pV_{dc} = \frac{1}{C_{eq}V_{dc}}[P_{conv1} - P_{conv2}] \tag{2}$$

$$C_{eq} = C.V_{dcbase}^2/VA_{base}$$

where C = DC capacitor magnitude and p is the differential operator.

Using the representation of P_{conv1} (eqn. 1) and P_{conv2} (eqn. 21, in the Appendix) in (eqn. 2) the dynamics of the DC link is

$$pV_{dc} = \frac{1}{C_{eq}V_{dc}}\left[|V_s|.I_s - B_{se}\rho|V_s||V_r|\sin(\theta_{sr} + \alpha) + B_{se}\rho|V_s|^2\sin(\alpha)\right] \tag{3}$$

The injection model of Fig. 3 is used to modify the admittance matrix (Y-Bus) of the multi-machine power network. The controllable loads at the sth and rth bus of the UPFC is

$$L_s = \frac{(P_s - jQ_s)}{|V_s|^2} \qquad L_r = \frac{(P_r - jQ_r)}{|V_r|^2} \tag{4}$$

These controllable admittances are added to the Y_{ss} and Y_{rr} elements of the Y-Bus matrix of the power network with UPFCs for the simulation.

The reactance of transmission line controls the real power flow. Thus the component (V_{cr}) of the series injection voltage in quadrature with the line current is generated from real power deviation ($P_{ref} - P$) in the transmission line after the series transformer. The in-phase component (V_{cp}) is either generated from the reactive power deviation ($Q_{ref} - Q$) in the transmission line or the voltage deviation ($V_{ref} - V$) of the bus after the series transformer. We have considered only the reactive power deviation in this paper. The magnitude ratio (ρ) and the phase difference (α) are calculated as

$$\rho = \frac{\sqrt{V_{cp}^2 + V_{cr}^2}}{|V_s|}$$

and

$$\alpha = \tan^{-1}\left(\frac{V_{cr}}{V_{cp}}\right) - \tan^{-1}\left(\frac{i_{rd}}{i_{rq}}\right) + \tan^{-1}\left(\frac{V_{sd}}{V_{sq}}\right) \tag{5}$$

where i_{rd} and i_{rq} are the d-axis and q -axis transmission line currents after the series transformer. V_{sd} and V_{sq} are the d -axis and q -axis voltage of the sth bus of UPFC. The detailed phasor diagram in the d–q reference frame is shown in Fig. 4.

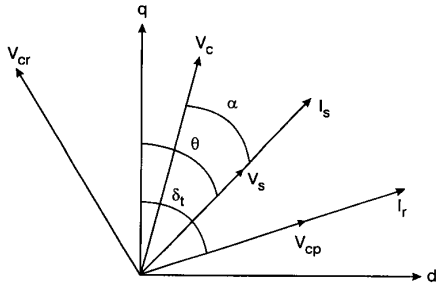

Fig. 4 *Phasor diagram*

To maintain the DC capacitor voltage constant, a PI controller is used in the following way to control the shunt current:

$$I_s = \left(K_{pdc} + \frac{K_{idc}}{p}\right)\Delta V_{dc} \tag{6}$$

where $\Delta V_{dc} = (V_{dcref} - V_{dc})$

3 Design of TS fuzzy controller for UPFC

As shown in the literature, regardless of the type, fuzzy controllers are just conventional non-linear controllers and can produce satisfactory results when constructed properly by trial and error. The Takagi-Sugeno (TS) fuzzy controller differs from the Mamdani type in its rule consequent. The linguistic rule consequent is made variable by means of its parameters. As the rule consequent is variable, the TS fuzzy control scheme can produce an infinite number of gain variation characteristics. In essence, the TS fuzzy controller is capable of offering more and better solutions to a wide variety of non-linear control problems. The active (V_{cp}) and reactive (V_{cr}) components of the series voltage source are controlled by reactive and active power deviation respectively. The active and reactive power deviations are fuzzified using two input fuzzy sets P (positive) and N (negative). The membership function used for the positive set is

$$\mu_P(x_i) = \begin{cases} 0 & x_i < -L \\ \frac{x_i+L}{2L} & -L \le x_i \le L \\ 1 & x_i > L \end{cases} \quad (7)$$

where $x_i(k)$ denotes the input to the fuzzy controller at the kth sampling instant given by

$$x_1(k) = e(k) = P_{ref} - P \quad \text{or} \quad Q_{ref} - Q \quad \text{and}$$
$$x_2(k) = \int e(k) \quad \text{or} \quad \dot{e}(k) \quad (8)$$

For the negative set,

$$\mu_N(x_i) = \begin{cases} 1 & x_i < -L \\ \frac{-x_i+L}{2L} & -L \le x_i \le L \\ 0 & x_i > L \end{cases} \quad (9)$$

The membership functions for x_1 and x_2 are shown in Figs. 5*a* and *b* respectively. The values of L_1 and L_2 are chosen on the basis of the maximum value of real or reactive power error, its integral or derivative. The TS fuzzy controller uses the four simplified rules as

R_1: If $x_1(k)$ is P and $x_2(k)$ is P then $u_1(k) = K_1(a_1.x_1(k) + a_2.x_2(k) + a_3.x_1(k).x_2(k))$

R_2: If $x_1(k)$ is P and $x_2(k)$ is N then $u_2(k) = K_2u_1(k)$

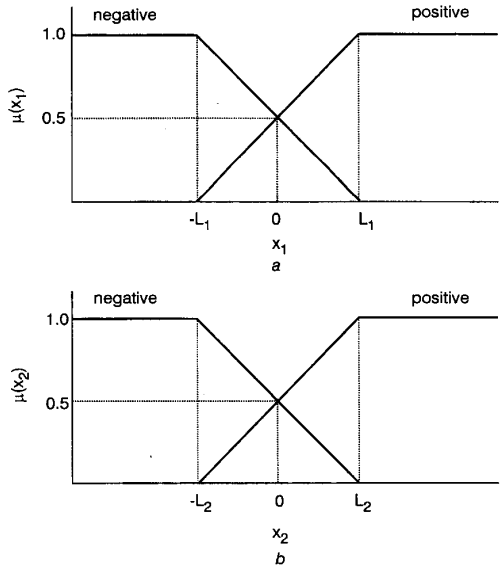

Fig. 5 *Membership function*
a x_1
b x_2

R_3: If $x_1(k)$ is N and $x_2(k)$ is P then $u_3(k) = K_3u_1(k)$

R_4: If $x_1(k)$ is N and $x_2(k)$ is N then $u_4(k) = K_4u_1(k)$

In the above rule base u_1, u_2, u_3, u_4 represent the consequent of the TS fuzzy controller. Using Zadeh's rules for AND operation and the general defuzzifier, the output of the TS fuzzy controller is

$$u(k) = \frac{\sum_{j=1}^{4} (\mu_j)^\gamma u_j(k)}{\sum_{j=1}^{4} (\mu_j)^\gamma} \quad (10)$$

However, for $\gamma = 1$, we get the centroid defuzzifier with $u(k)$ given by

$$u(k) = a.x_1(k) + b.x_2(k) + c.x_1(k).x_2(k) \quad (11)$$

where

$$a \triangleq a_1K, \quad b = a_2K, \quad c = a_3K$$

and

$$K = K_1(\mu_1 + K_2\mu_2 + K_3\mu_3 + K_4\mu_4)/(\mu_1 + \mu_2 + \mu_3 + \mu_4) \quad (12)$$

The value of $\int e(k)$ is taken as the sum $\Sigma e(k)$ and $\dot{e}(k)$ as difference $\Delta e(k)$ for implementing the control. The two control schemes with either sum of error ($\Sigma e(k)$) or difference of error ($\Delta e(k)$) are shown in Figs. 6 and 7, respectively. The above TS fuzzy controller is a highly non-linear variable gain controller and the coefficients a_1, a_2, a_3 produce wide variations of the controller gain.

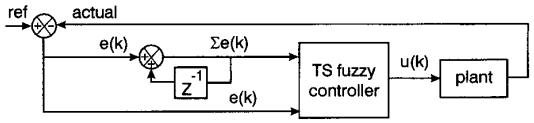

Fig. 6 *TS fuzzy control scheme with error and integral of error*

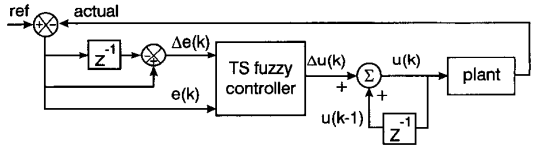

Fig. 7 *TS fuzzy control scheme with error and derivative of error*

In the case where the PI regulator is used in controlling V_{cp} and V_{cr}, the equations are:

$$V_{cp} = \left(K_{pp} + \frac{K_{ip}}{p}\right)\Delta Q$$
$$V_{cr} = \left(K_{pr} + \frac{K_{ir}}{p}\right)\Delta P \quad (13)$$

where $\Delta P = (P_{ref} - P)$, $\Delta Q = (Q_{ref} - Q)$.

4 Simulation results

The performance of the TS fuzzy controller in damping the inter-area mode (difference in speed of machine-2 and machine-1) and local mode (difference in speed of machine-2 and machine-3) was tested on a multi-machine power system (Fig. 1) subjected to a variety of transient disturbances such as faults at different locations, sudden change in local loads, change in mechanical power input, etc. The loading of the three machines are $P_1 = 4.4120$, $Q_1 = 1.9634$, $P_2 = 1.3$, $Q_2 = 0.1$, $P_3 = 1.3$ and $Q_3 = 0.15$, p.u. The machine M-1 is chosen as the reference machine. The system response to different disturbances is shown to evaluate the performance of the controller in comparison to the conven-

tional PI controller. The system data is provided in Appendix 3. A modulating signal based on the algebraic sum of the difference in speed between the machines M-1 and M-2, and M-2 and M-3, and is used to damp the power system oscillations. In that case the signal ΔP is to be replaced by

$$\Delta P + K_{\omega 1}(\omega_2 - \omega_1) + K_{\omega 2}(\omega_3 - \omega_1) \qquad (14)$$

for UPFC-1 and by

$$\Delta P + K_{\omega 3}(\omega_3 - \omega_2) \qquad (15)$$

for UPFC-2.

The parameters of the TS fuzzy controller and PI controller for both the UPFCs are given in Appendix 3. The coefficients of the auxiliary signal used in eqns. 14 and 15 are optimised at $K_{\omega 1} = 1.0$, $K_{\omega 2} = 0.5$, $K_{\omega 3} = 1.4$, by trial and error. The proportional and integral gains of the DC voltage regulator of UPFC-1 are chosen to be 2.0 and 10.0 and those of UPFC-2 are 0.5 and 2.0 respectively.

The TS fuzzy control scheme with integral of error (Fig. 6) is termed as TSINT and that with derivative (Fig. 7) as TSDER.

4.1 Case 1

A three-phase fault of 100ms duration is simulated at the middle of the transmission line connecting Bus-2 and Bus-4. The performance of the fuzzy controller, PI controller and without a UPFC in the network are shown in Figs. 8–11. From Figs. 8 and 9, the superiority of the TSINT fuzzy controller with auxiliary signal is well marked in damping inter-area and local mode oscillations. Figs. 10 and 11 depict the variation of DC capacitor voltage of UPFC-1 and UPFC-2, respectively. The variation of voltage across the DC capacitor is well controlled even by a PI controller. DC capacitor voltage is a very important factor for successful operation of the series and shunt converters.

4.2 Case 2

With the same operating conditions of the network, a three-phase fault of 100ms duration is simulated at the middle of one of the transmission lines connecting Bus-6 and Bus-1. The performance of the TSINT fuzzy with and without auxiliary control signals and conventional PI regulators is depicted in Fig. 12 (inter-area mode) and Fig. 13 (local mode). The performance without an auxiliary signal controller is presented to establish the damping property of the auxiliary signal. Figs. 14 and 15 present the variation of the DC voltage during a transient disturbance.

4.3 Case 3

The load admittance at Bus-4 is suddenly decreased by 95% for 100ms duration. This simulates a large load disturbance. The inter-area and local modes of oscillations are presented in Figs. 16 and 17 respectively for PI and TSINT control schemes. The PI controller performs badly in this case also. Fig. 18 shows the variation of the DC voltage of the connecting capacitor of UPFC-1. The DC voltage excursion of UPFC-2 is observed to be within 0.2% for both the control schemes.

4.4 Case 4

The mechanical torque input of M-1 is increased by 30% for 100ms and then brought back to the original value. The inter-area and local modes of oscillations for the transient disturbance are depicted in Figs. 19 and 20, respectively for PI and TSINT fuzzy controller. Fig. 21 presents the DC voltage excursions of UPFC-1 during transient. In this case the DC voltage excursions of UPFC-2 is also within 0.2%.

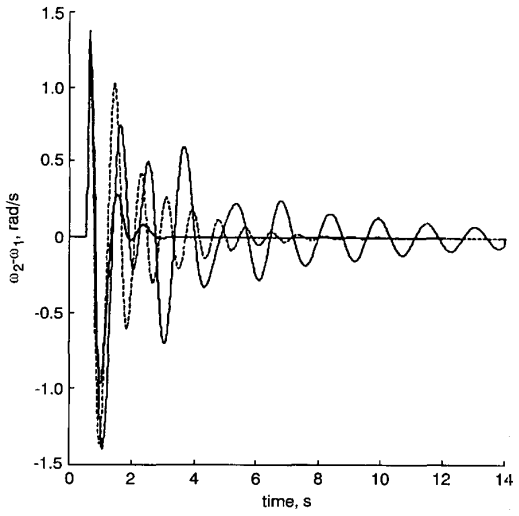

Fig. 8 *Inter-area mode oscillations*
---- PI (with auxiliary signal)
—— no UPFC
▬▬ TSINT (with auxiliary signal)

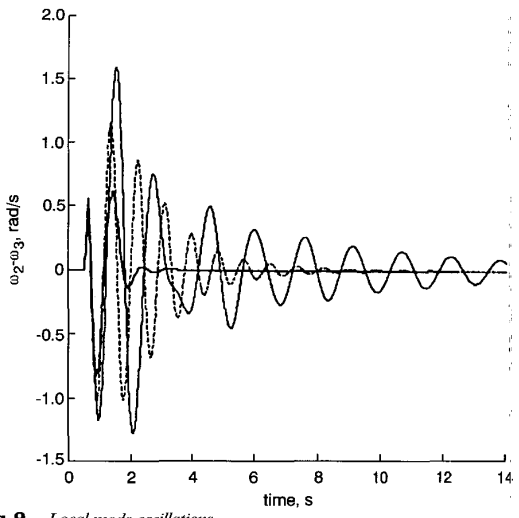

Fig. 9 *Local mode oscillations*
---- PI (with auxiliary signal)
—— no UPFC
▬▬ TSINT (with auxiliary signal)

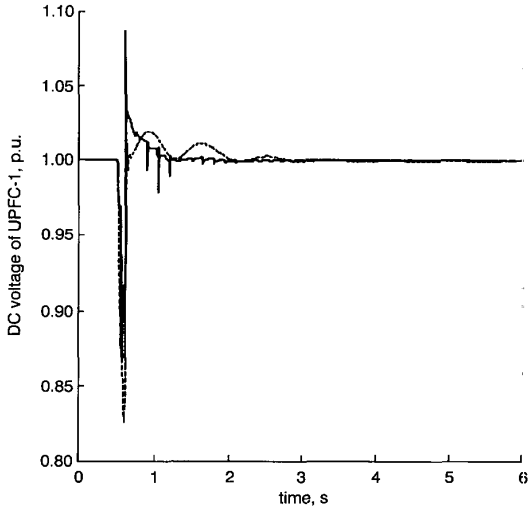

Fig. 10 *DC voltage excursions of UPFC-1*
---- PI (with auxiliary signal)
▬▬ TSINT (with auxiliary signal)

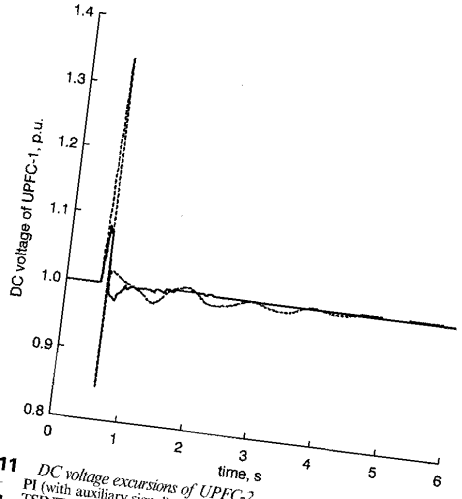

Fig. 11 *DC voltage excursions of UPFC-2*
PI (with auxiliary signal)
TSINT (with auxiliary signal)

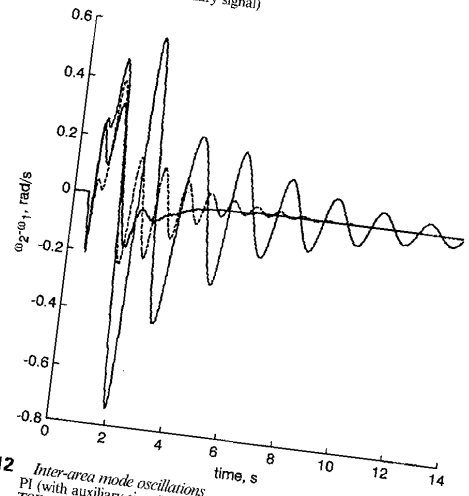

Fig. 12 *Inter-area mode oscillations*
PI (with auxiliary signal)
TSINT (without auxiliary signal)
TSINT (with auxiliary signal)

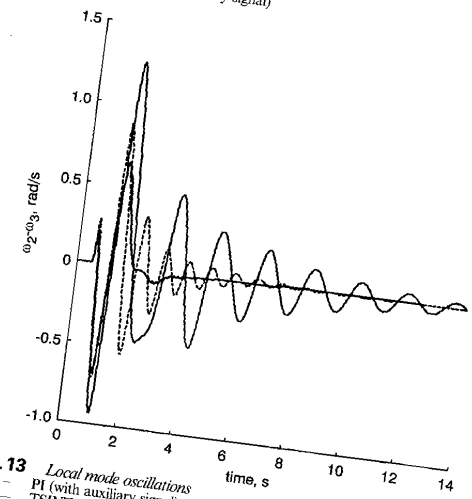

Fig. 13 *Local mode oscillations*
PI (with auxiliary signal)
TSINT (without auxiliary signal)
TSINT (with auxiliary signal)

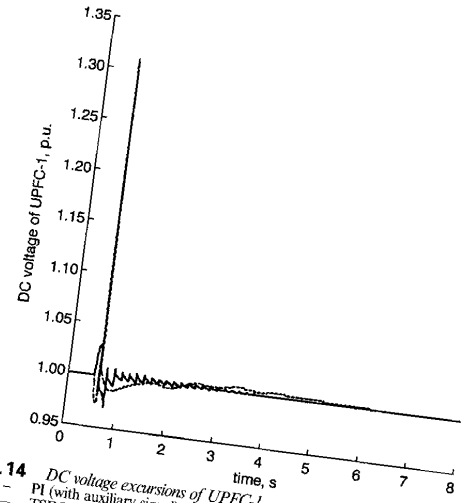

Fig. 14 *DC voltage excursions of UPFC-1*
PI (with auxiliary signal)
TSINT (without auxiliary signal)

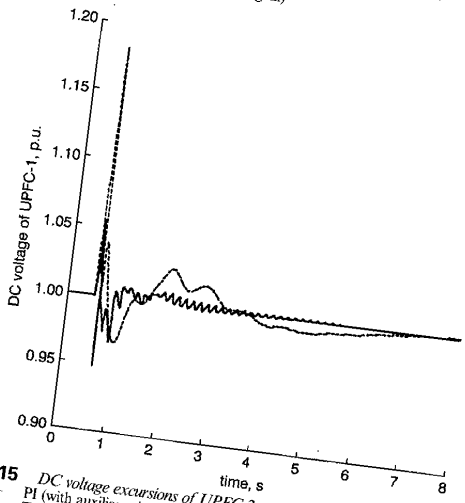

Fig. 15 *DC voltage excursions of UPFC-2*
PI (with auxiliary signal)
TSINT (with auxiliary signal)

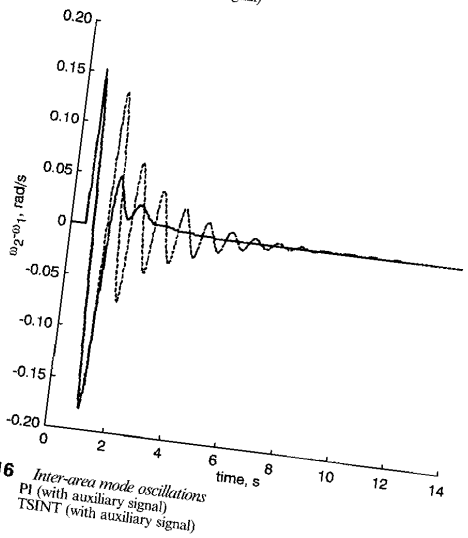

Fig. 16 *Inter-area mode oscillations*
PI (with auxiliary signal)
TSINT (with auxiliary signal)

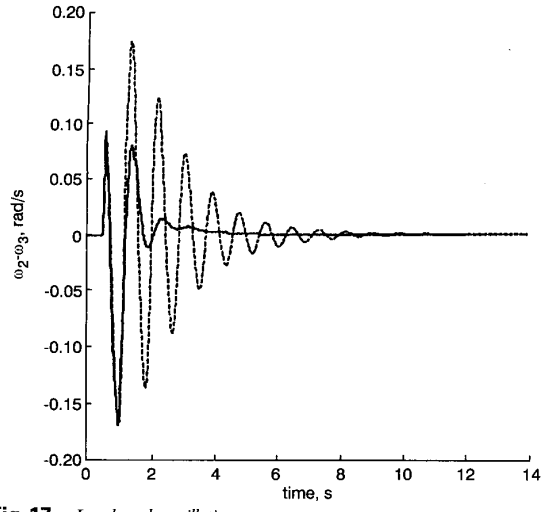

Fig. 17 *Local mode oscillations*
---- PI (with auxiliary signal)
—— TSINT (with auxiliary signal)

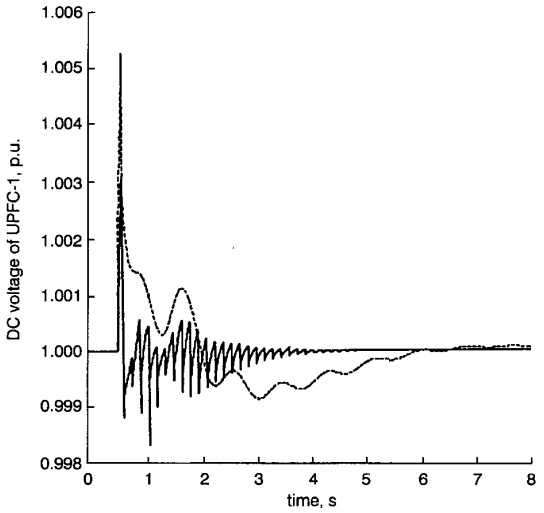

Fig. 18 *DC voltage excursions of UPFC-1*
---- PI (with auxiliary signal)
—— TSINT (with auxiliary signal)

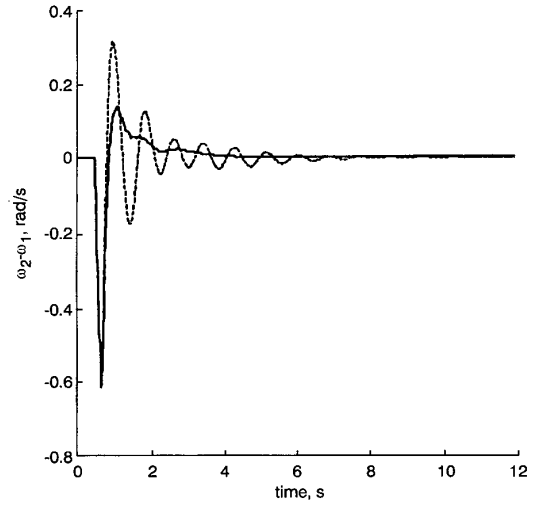

Fig. 19 *Inter-area mode oscillations*
---- PI (with auxiliary signal)
—— TSINT (with auxiliary signal)

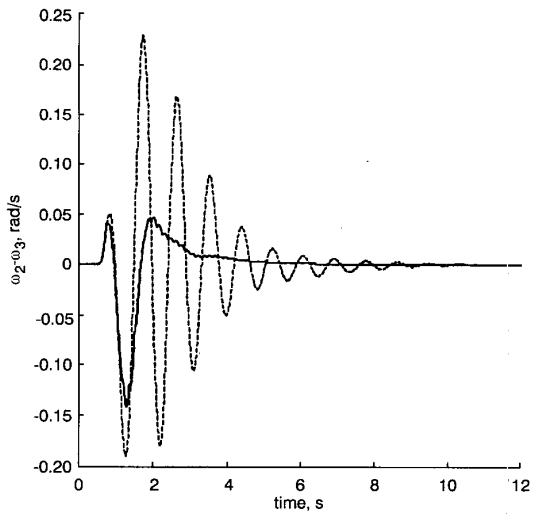

Fig. 20 *Local mode oscillations*
---- PI (with auxiliary signal)
—— TSINT (with auxiliary signal)

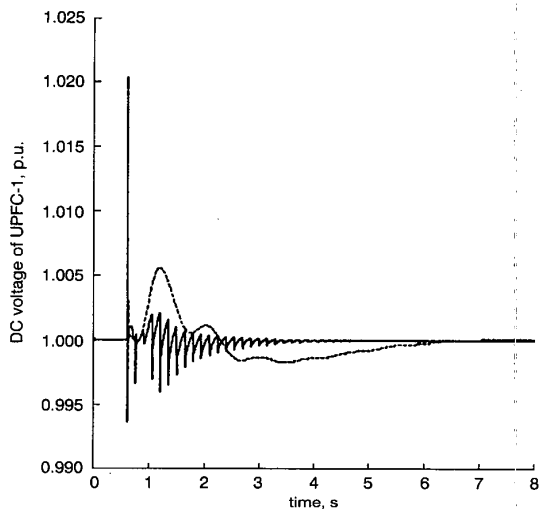

Fig. 21 *DC voltage excursions of UPFC- 1*
---- PI (with auxiliary signal)
—— TSINT (with auxiliary signal)

4.5 Case 5

To compare the performance of integral and derivative types of TS fuzzy controller of Figs. 6 and 7, the fault as in case-1 is considered. The parameters of both the TS fuzzy controllers are identical, except for the membership function used for $x_2(k)$. The inter-area and local modes of oscillations are depicted in Figs. 22 and 23 respectively. The first swing of the inter-area mode is decreased for the derivative type, but the performances of both types are the same for local mode oscillations. The voltage excursions of both DC link capacitors are found to be almost the same in both of the fuzzy control schemes.

4.6 Case 6

To get an idea about the different control schemes of the TS fuzzy controller, another case is considered. The fault of case-2 is simulated for both of the controllers. The inter-area and local modes of oscillations are presented in Figs. 24 and 25 respectively. The derivative type has a larger first swing in the inter-area mode. The local mode of oscillations is virtually the same for both of the schemes.

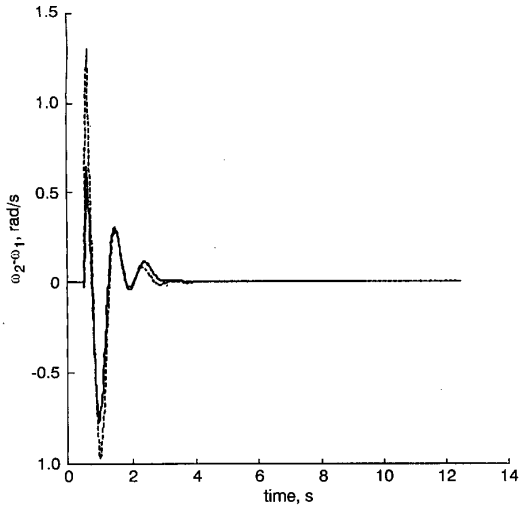

Fig. 22 *Inter-area mode oscillations*
---- TSINT (with auxiliary signal)
——— TSDER (with auxiliary signal)

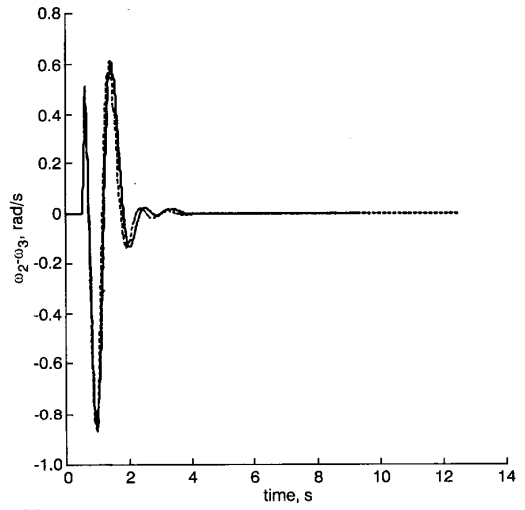

Fig. 23 *Local mode oscillations*
---- TSINT (with auxiliary signal)
——— TSDER (with auxiliary signal)

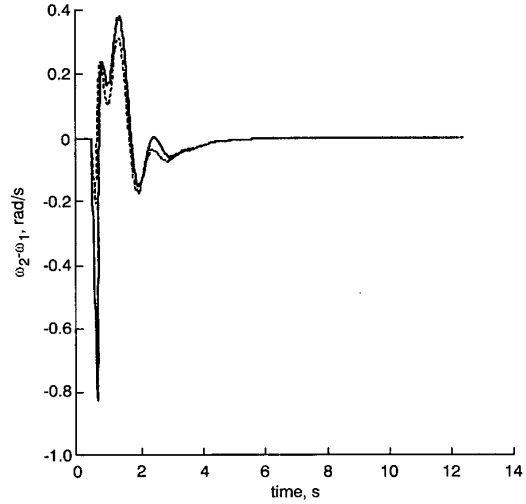

Fig. 24 *Inter-area mode oscillations*
---- TSINT (with auxiliary signal)
——— TSDER (with auxiliary signal)

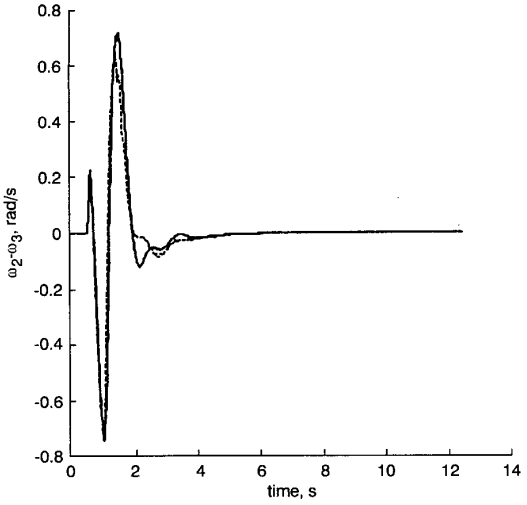

Fig. 25 *Local mode oscillations*
---- TSINT (with auxiliary signal)
——— TSDER (with auxiliary signal)

The DC link voltage oscillations of UPFC-1 and UPFC-2 are also the same for the two schemes.

5 Conclusions

A new non-linear fuzzy controller with a wide ranging gain variation has been proposed for the voltage source inverter control of an UPFC in a multi-machine power system. The UPFC using the proposed control scheme provides significant improvement in damping the electromechanical oscillations of the generators. Both local mode and inter-area mode oscillations show significant reduction in their first and subsequent swings for this controller in comparison to the conventional PI control. The TS fuzzy controllers offer a basis for using expert control knowledge and experience in the form of fuzzy control rules, membership functions and fuzzy logic to construct a variety of non-linear variable gain controllers with desired gain variation characteristics. The initial adjustment of the parameters of the new TS fuzzy controller, however, requires some trial and error, although new optimisation schemes have been proposed recently. Finally, several fault and load disturbance results have been presented to highlight the effectiveness of the proposed FACTS controller.

6 References

1 GYUGYI, L.: 'Unified power flow concept for flexible AC transmission systems', *IEE Proc. C*, 1992, **139**, (4), pp. 323–332
2 PADIYAR, K.R., and KULKARNI, A.M.: 'Control design and simulation of unified power flow controller', *IEEE Trans.*, 1998, **PWRD–13**, (4), pp. 1348–1354
3 HSU, Y., and CHENG, C.: 'Design of fuzzy power system stabilizers for multi-machine power systems', *IEE Proc. C*, 1990, **137**, (2), pp. 233–238
4 HASSAN, M.A.M., MALIK, O.P., and HOPE, G.S.: 'A fuzzy logic based stabilizer for a synchronous machine', *IEEE Trans.*, 1991, **EC–6**, (3), pp. 407–414
5 HASSAN, M.A.M., and MALIK, O.P.: 'Implementation and laboratory test results for a fuzzy logic based self-tuned PSS', *IEEE Trans.*, 1993, **EC–8**, (2), pp. 221–228
6 DASH, P.K., MISHRA, S., and LIEW, A.C.: 'Fuzzy-logic-based VAR stabiliser for power system control', *IEE Proc. C*, 1995, **142**, (6), pp. 618–624
7 NOROOZIAN, M., ANDERSON, G., and TOMSOVIC, K.: 'Robust, near time-optimal control of power system oscillations with fuzzy logic', *IEEE Trans.*, 1996, **PWRD–11**, (1), pp. 393–400
8 LIMYINGCHAROEN, S., ANNAKKAGE, U.D., and PAHALAWATHTHA, N.C.: 'Fuzzy logic based unified power flow controllers for transient stability improvement', *IEE Proc. Gener. Trans. Distr.*, 1998, **145**, (3), pp. 225–232

9 YING, H.: 'Constructing non-linear variable gain controllers via the Takagi-Sugeno fuzzy control', *IEEE Trans. Fuzzy Syst.*, 1998, **6**, (2), pp. 226–235
10 NOROOZIAN, M., ANGQUIST, L., GHANDARI, M., and ANDERSON, G.: 'Improving power system dynamics by series-connected FACTs devices', *IEEE Trans.*, 1997, **PWRD–12**, (4), pp. 1635–1641

7 Appendices

7.1 Appendix 1

The dynamics of each synchronous machine is modelled by three differential equations given by

$$\omega = \omega_0 + p\delta, \quad p = d/dt \text{ (differential operator)}$$

$$p\omega = \frac{\pi f}{H}(P_m - P_e)$$

$$pe'_q = \left(E_{fd0} + \Delta E_{fd} - e'_q - (x_d - x'_d)i_d\right)/\tau'_{d0}$$

$$p\Delta E_{fd} = K_e(V_{ref} - V_t)/\tau_e - \Delta E_{fd}/\tau_e$$

$$\text{and } -6.0 \leq E_{fd} \leq 6.0$$

$$P_e = e'_q i_q + (x_q - x'_d)i_d i_q$$

The structure of the PSS used in machine-2 is

$$K_\delta \cdot \frac{sT_Q}{1+sT_Q}\left(\frac{1+sT_1}{1+sT_2}\right)$$

where $K_\delta = 0.24$, $T_Q = 0.4$, $T_1 = 0.3$ and $T_2 = 0.3$.

7.2 Appendix 2

Let an ideal series connected voltage source of magnitude V_c and reactance X_{se} be present between two buses (s, r) in a power system as shown in Fig. 26.

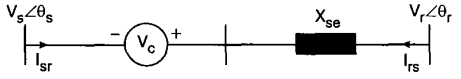

Fig. 26 *Voltage source representation of series converter*

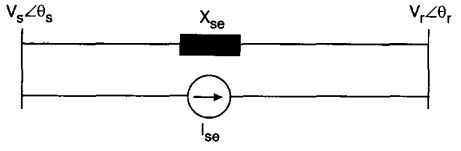

Fig. 27 *Current source representation of series converter*

The Norton's equivalent of the above circuit is represented in Fig. 27.

$I_{se} = -j\,B_{se}V_c$ in parallel with the line where $B_{se} = 1/X_{se}$.

The current source I_{se} corresponds to the injection powers S_s and S_r where:

$$S_s = V_s(-I_{se})^* \tag{16}$$

$$S_r = V_r(I_{se})^* \tag{17}$$

The injection power S_s and S_r are simplified to

$$S_s = V_s\left(jB_{se}\rho V_s e^{j\alpha}\right)^*$$
$$= -B_{se}\rho|V_s|^2\sin(\alpha) - jB_{se}\rho|V_s|^2\cos(\alpha) \tag{18}$$

$$S_r = V_r\left(-jB_{se}\rho V_s e^{j\alpha}\right)^*$$
$$= B_{se}\rho|V_s|.|V_r|\sin(\theta_{sr}+\alpha)$$
$$+ jB_{se}\rho|V_s|.|V_r|\cos(\theta_{sr}+\alpha) \tag{19}$$

where $V_c = \rho V_s e^{j\alpha}$ and $\theta_{sr} = \theta_s - \theta_r$.

Based on the explanation above the injection model of a series connected voltage source can be represented by two dependent loads as shown in Fig. 28.

Fig. 28 *Equivalent representation of series converter in load form*
$P_s = \rho B_{se}|V_s|^2\sin(\alpha)$ $\quad P_r = -\rho B_{se}|V_s|.|V_r|\sin(\theta_{sr}+\alpha)$
$Q_s = \rho B_{se}|V_s|^2\cos(\alpha)$ $\quad Q_r = -\rho B_{se}|V_s|.|V_r|\cos(\theta_{sr}+\alpha)$

The apparent power supplied by the series voltage source converter is

$$S_{conv2} = V_c I^*_{sr} = \rho e^{j\alpha}V_s\left(\frac{V_s + V_c - V_r}{jX_{se}}\right)^* \tag{20}$$

$$P_{conv2} = B_{se}\rho|V_s|.|V_r|\sin(\theta_{sr}+\alpha) - B_{se}\rho|V_s|^2\sin(\alpha) \tag{21}$$

$$Q_{conv2} = -B_{se}\rho|V_s|.|V_r|\cos(\theta_{sr}+\alpha) + B_{se}\rho|V_s|^2\cos(\alpha) + B_{se}\rho|V_s|^2 \tag{22}$$

7.3 Appendix 3

Table 1: Generator data (P_{base} = 1000MVA)

Equivalent gen.	Generator-1	Generator-2	Generator-3
Type	Thermal	Hydro	Hydro
Capacity	5500 MVA	1800 MVA	1800 MVA
Inertia constant (H)	4s	4s	4s
d-axis reactance (X_d)	2.00p.u.	1.00p.u.	1.00p.u.
q-axis reactance (X_q)	1.90p.u.	0.60p.u.	0.60p.u.
d-axis transient reactance (X'_d)	0.25p.u.	0.30p.u.	0.30p.u.
Field time constant (τ'_{od})	6.00p.u.	6.00p.u.	6.00p.u.
AVR gains (K_e)	30	10	10
AVR time constant (τ_e)	0.05s	0.05s	0.05s

Transmission lines (double circuit)
L = 350km, x = 0.20Ω/km (compensated line)
L_2 = 50km, x = 0.34Ω/km, L_3 = 50km, x = 0.34Ω/km
Loads (p.u.) in admittance form
Y_{L1} = 6.0 – j1.2, Y_{L2} = 0.1 – j0.010, Y_{L3} = 0.1 – j0.010, Y_{L4} = 1.0 – j0.2
UPFC data
V_{dcbase} = 31.113kV, C = 5500μF
x_{se} = 0.007, ρ_{max} = 0.18, ρ_{min} = –0.18
Controller data
Both TSINT and TSDER
a_{1p1} = 0.25, a_{2p1} = 0.1, a_{3p1} = –0.01, a_{1r1} = 0.05, a_{2r1} = 0.05, a_{3r1} = –0.01, a_{1p2} = 0.15, a_{2p2} = 0.15, a_{3p2} = –0.01, a_{1r2} = 0.05, a_{2r2} = 0.05, a_{3r2} = –0.01, K_{1p1} = 0.1, K_{2p1} = 0.05, K_{3p1} = 0.05, K_{4p1} = 0.1, K_{1r1} = 0.1, K_{2r1} = 0.05, K_{3r1} = 0.05, K_{4r1} = 0.1, K_{1p2} = 0.1, K_{2p2} = 0.05, K_{3p2} = 0.05, K_{4p2} = 0.1, K_{1r2} = 0.1, K_{2r2} = 0.05, K_{3r2} = 0.05, K_{4r2} = 0.1, L_{1p1} = 2.0, L_{1r1} = 2.0, L_{1p2} = 2.0, L_{1r2} = 2.0 and γ = 0.5.
TSINT
L_{2p1} = 10, L_{2r1} = 50, L_{2p2} = 10, L_{2r2} = 50
TSDER
L_{2p1} = 2, L_{2r1} = 2, L_{2p2} = 2, L_{2r2} = 2
PI controller
K_{pp1} = 0.01, K_{ip1} = 0.4, K_{pr1} = 0.01, K_{ir1} = 0.4, K_{pp2} = 0.01, K_{ip2} = 0.04, K_{pr2} = 0.01, K_{ir2} = 0.4
The second subscript of all parameters in the controller data either corresponds to in phase (p) or reactive (r) voltage component and the third to the UPFC number.